Article

# Ligand-controlled stereodivergent alkenylation of alkynes to access functionalized *trans*- and *cis*-1,3-dienes

Tianyu Long[1,3], Chen Zhu [2,3], Ling Li[1], Liang Shao[1], Shengqing Zhu[1], Magnus Rueping [2] ✉ & Lingling Chu [1] ✉

Precise stereocontrol of functionalized alkenes represents a long-standing research topic in organic synthesis. Nevertheless, the development of a catalytic, easily tunable synthetic approach for the stereodivergent synthesis of both *E*-selective and even more challenging *Z*-selective highly substituted 1,3-dienes from common substrates remains underexploited. Here, we report a photoredox and nickel dual catalytic strategy for the stereodivergent sulfonylalkenylation of terminal alkynes with vinyl triflates and sodium sulfinates under mild conditions. With a judicious choice of simple nickel catalyst and ligand, this method enables efficient and divergent access to both *Z*- and *E*-sulfonyl-1,3-dienes from the same set of simple starting materials. This method features broad substrate scope, good functional compatibility, and excellent chemo-, regio-, and stereoselectivity. Experimental and DFT mechanistic studies offer insights into the observed divergent stereoselectivity controlled by ligands.

1,3-Dienes are one of the most important structural motifs frequently found in many natural products and biologically active compounds[1,2], as well as serve as valuable building blocks for diverse transformations in organic synthesis[3,4]. Accordingly, the stereoselective synthesis of 1,3-dienes has received paramount attention in organic synthesis[5-7]. Olefinations of carbonyls are widely embraced methods to access 1,3-dienes, while typically leading to *E/Z* isomers[8,9]. Alternatively, transition-metal-catalyzed cross-coupling reactions, including Heck couplings[10], ene-yne couplings[11], hydrovinylation of alkynes[12], alkenyl-alkenyl couplings[13-15], and boroalkenylation of alkynes[16-19], have emerged as a powerful strategy for the stereoselective synthesis of 1,3-dienes. Despite enabling, these methods generally lead to thermodynamically more stable *E*-isomers, or rely on the use of stereochemically well-defined organometallic agents or electrophiles. To the best of our knowledge, catalytic stereodivergent protocol that would enable both *E*-selective and even more challenging *Z*-selective access of highly substituted 1,3-dienes from one set of substrates remains underexploited[20,21].

Ni-catalyzed vicinal difunctionalization of alkynes via metalation followed by subsequent functionalization of alkenyl nickel species represents an attractive strategy for the synthesis of substituted alkenes from simple starting materials[22-26]. The highly stereoselective metalation step ensures the selective construction of *syn*-addition products, with a few exceptions of *anti*-selective examples that proceed via substrate-driving *E/Z* isomerization of alkenyl nickel species[27-34]. Recently, radical-involved catalytic 1,2-difunctionalization of alkynes has been disclosed to furnish trisubstituted alkenes with complementary *anti*-selectivity[35-42]. Particularly, utilizing dual nickel/photoredox catalysis[43-47] has further exploited a number of selective difunctionalization of alkynes with diverse coupling partners under mild conditions[48-56]. Nevertheless, rare examples for stereodivergent synthesis of both *trans*- and *cis*-substituted alkenes from alkynes are reported. Recently, we reported a photoredox/nickel dual catalyzed stereodivergent difunctionalization of alkynes, furnishing both *syn*- and *anti*-selective aryl-substituted alkenes via the judicious choice of

[1]State Key Laboratory for Modification of Chemical Fibers and Polymer Materials, Center for Advanced Low-Dimension Materials, Donghua University, College of Chemistry and Chemical Engineering, Shanghai 201620, China. [2]King Abdullah University of Science and Technology (KAUST), KAUST Catalysis Center (KCC), Thuwal 23955-6900, Saudi Arabia. [3]These authors contributed equally: Tianyu Long, Chen Zhu. ✉e-mail: magnus.rueping@kaust.edu.sa; lingling.chu1@dhu.edu.cn

photocatalysts with different triplet state energies (Fig. 1a)[57]. Despite attractive, such a *contra*-thermodynamic alkene isomerization strategy relies on the structure of alkenes or photocatalysts. Thus, the development of photoredox/nickel dual-catalyzed divergent method with a complementary stereoselective tuning strategy to access more diverse types of alkenes, such as functionalized *cis*- and *trans*-1,3-dienes, under mild and operationally simple conditions would be of particular interest.

Here, we show a ligand-controlled stereodivergent alkenyl-functionalization of alkynes with vinyl triflates and sodium sulfinates via photoredox and nickel dual catalysis (Fig. 1b). This strategy furnishes a wide array of synthetically valuable *cis*- and *trans*-sulfonyl-1,3-dienes[58,59] in one pot from simple starting materials. Detailed mechanistic experiments and computational investigations offer insights into the origins of the observed stereoselectivity and the role of dynamic ligand exchange in the dual ligand system.

## Results and discussion
### Reaction optimizations
Our investigations were started with phenylacetylene **1**, vinyl triflate **2**, and sodium *p*-tolylsulfinate **3** as model substrates (Table 1). After some experimentations, we found that in the presence of Ru(dtbbpy)$_3$(PF$_6$)$_2$ as the photocatalyst, Ni(OAc)$_2$•4H$_2$O as the nickel catalyst, and 1,10-phenanthroline (1,10-phen) as the ligand, irradiation of the reaction mixture in DMF with blue LEDs gave the sulfonylated diene product **4b** in 45% yield with excellent regio- and *anti*-selectivity (entry 1). Pleasingly, employing terpyridine (tpy) as the ligand dramatically improved the yield of product **4b** to 86% without observation of *syn*-selective isomer (entry 2). Further evaluation of nickel catalysts or pre-catalysts disclosed that Ni(OAc)$_2$•4H$_2$O was the optimal catalyst for this *anti*-selective transformation (entries 3-6). During this process, we noticed that the nature of nickel salts played an intriguing effect on the *trans/cis* selectivity. Switching to phosphine-ligated nickel pre-catalysts resulted in the formation of a mixture of *trans/cis* isomers **4a** and **4b** in varied yields and *Z/E* ratios (entries 4-6). Interestingly, the use of

NiCl$_2$•dppf in the absence of terpyridine led to the exclusive formation of *syn*-selective product **4a**, albeit in low yield (entry 7). The addition of 1,10-phen as an exogenous ligand turned out to be beneficial to the yield of **4b**, together with the formation of isomer **4a** (entry 8)[60]. Careful examination of the ratio of nickel and ligand revealed that the use of 20 mol% NiCl$_2$•dppf with 10 mol% 1,10-phen furnished **4a** in 80% yield with excellent *cis/trans* selectivity (entries 8-11). Finally, control experiments disclosed that photocatalyst, nickel catalyst, and light were all essential for this stereodivergent reaction (entries 12-14) (see Supplementary Information for more optimization details).

### Substrate scope studies
With the optimal reaction conditions in hand, we began to investigate the substrate compatibility of this stereodivergent protocol in the presence of Ru(dtbbpy)$_3$(PF$_6$)$_2$ with two sets of nickel catalysts (entries 2 and 11, respectively). As shown in Fig. 2, a series of cyclic vinyl triflates smoothly underwent cross-couplings with phenyl acetylene **1** and TsNa **3**, furnishing 1,3-dienyl sulfones with high efficiency and excellent *Z* or *E*-selectivity (**4a–18a** & **4b–18b**). Cyclohexenyl triflates with substituents on 4-position, including alkyl, aryl, ketal, and ester, were well compatible; interestingly, *ortho*-substituents turned out to be well-tolerated with any deleterious effect to the coupling yield and *cis/trans* selectivity (**10a** & **10b**). Moreover, vinyl triflates derived from heteroatom-incorporated cyclic ketones, represented by tetrahydro-4*H*-pyran-4-one and 4-piperidinone, were competent coupling partners, affording corresponding dienes with excellent selectivity (**12a-13a** & **12b-13b**). The reaction of cyclic vinyl triflates that were prepared from 5-, 7- and 8-membered cyclic ketones proceeded smoothly, albeit with slightly decreased *E/Z* selectivity in the case of 5-membered vinyl triflate (**14a-17a** & **14b-17b**). Pleasingly, acyclic vinyl triflates that derived from aliphatic ketones were suitable substrates, furnishing the diene products with excellent selectivity yet decreased yields (**18a-21a** & **18b-21b**). The reactions with 1,2-disubstituted vinyl triflates produced the desired coupling products with excellent *syn*-selectivity yet low *anti*-selectivity (**22a** & **22b**). It should be noted that
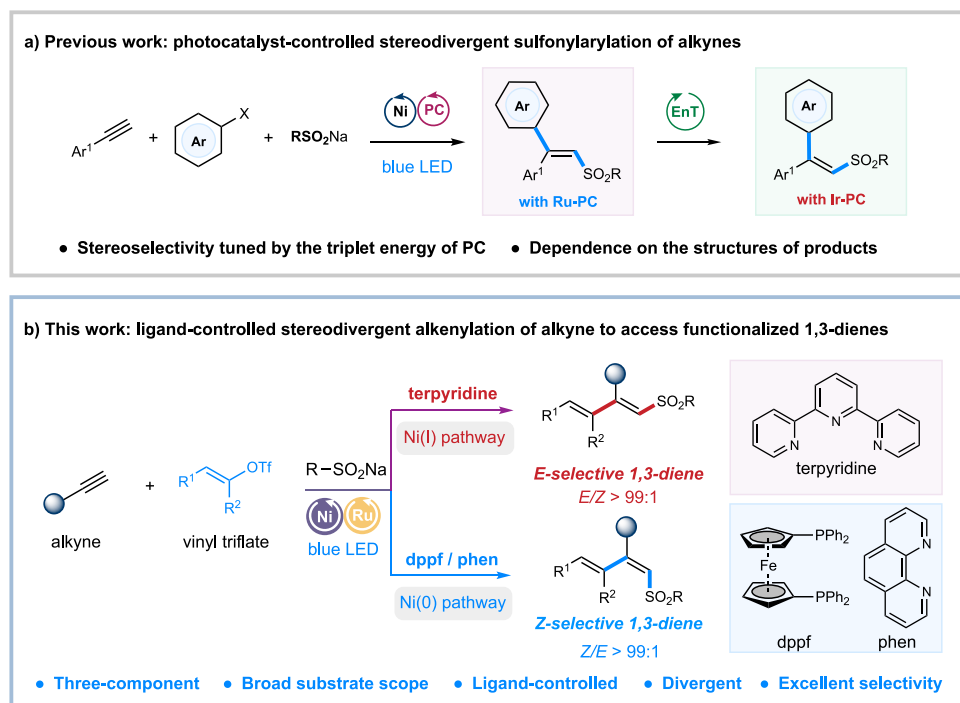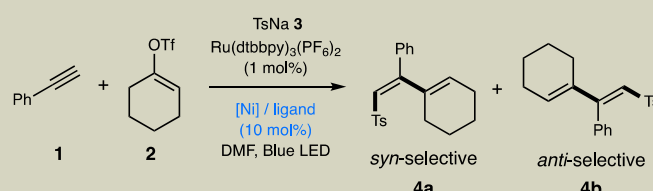


**Fig. 1 | Background and recent work of carbosulfonylation of alkynes.**
**a** Previous work: photocatalyst-controlled stereodivergent sulfonylarylation of alkynes. **b** This work: ligand-controlled stereodivergent alkenylation of alkynes to access functionalized 1,3-dienes. PC photocatalyst, EnT energy transfer, dppf 1,1-bis(diphenylphosphino)ferrocene, phen 1,10-phenanthroline.

## Table 1 | Optimization of reaction conditions[a]



| entry | nickel catalyst | ligand | yield of 4b | yield of 4a |
|---|---|---|---|---|
| 1 | Ni(OAc)$_2$·4H$_2$O | 1,10-phen | 45% | 0% |
| 2 | Ni(OAc)$_2$·4H$_2$O | tpy | 86% | 0% |
| 3 | NiCl$_2$ | tpy | 68% | 0% |
| 4 | NiCl$_2$·dppe | tpy | 10% | 2% |
| 5 | NiCl$_2$(PPh$_3$)$_2$ | tpy | 31% | 16% |
| 6 | NiCl$_2$·dppf | tpy | 28% | 10% |
| 7 | NiCl$_2$·dppf | – | 0% | 32% |
| 8 | NiCl$_2$·dppf | 1,10-phen | 15% | 51% |
| 9 | NiCl$_2$·dppf | 1,10-phen (15 mol%) | 13% | 46% |
| 10 | NiCl$_2$·dppf (15 mol%) | 1,10-phen | 5% | 53% |
| 11 | NiCl$_2$·dppf (20 mol%) | 1,10-phen | 0% | 80% |
| 12 | w/o PC | | 0% | 0% |
| 13 | w/o light | | 0% | 0% |
| 14 | w/o nickel | | 0% | 0% |

[a]Reactions conditions: Ru(dtbbpy)$_3$(PF$_6$)$_2$ (1 mol%), [Ni] (10 mol%), ligand (10 mol%), alkyne **1** (1.5 equiv.), vinyl triflate **2** (0.1 mmol), TsNa **3** (1.5 equiv.), DMF [0.04 M], 35 °C, blue LED, 6 h. Yields were determined by $^1$H-NMR using 1,3-benzodioxole as an internal standard. Z/E ratios were determined by $^1$H-NMR. tpy = terpyridine; 1,10-phen = 1,10-phenanthroline; dppf = 1,1'-bis(diphenyphosphino) ferrocene.

the structures of products **13a** and **13b** are validated by single-crystal X-ray diffraction and the stereoselectivity of the two isomers of products **4a** & **4b**, **13** & **13b**, **22a** & **22b**, **25a** & **25b**, and **53a** & **53b** is further confirmed by COSEY and NOSEY. The stereoselectivity of other products is assigned by analogy.

Next, we turned our attention to the scope of the alkyne component (Fig. 2). A wide range of aryl alkynes, bearing electron-donating or withdrawing substituents on the *ortho-*, *meta-*, or *para*-positions of aromatic rings, all underwent efficient couplings to furnish sulfonated 1,3-dienes with excellent stereoselectivity (**23a–37a** & **23b–37b**). The mild conditions were compatible with diverse functional groups, including esters, halides, phenols, and amines, leaving synthetic handles for further potential manipulations. Acetylenes incorporated with a heteroarene, represented by quinoline, thiophene, and dibenzo[*b,d*] furan, all worked well with high efficiency (**35a–36a, 38a** & **35b–36b, 38b**). Besides, aliphatic terminal alkynes were suitable substrates, affording functionalized 1,3-dienes in decreased yields yet with excellent Z/E selectivity (**39a–43a** & **39b–43b**). Nevertheless, the reaction of internal alkynes only proceeded with moderate *trans/cis* selectivity under these two reaction conditions (**44a** & **44b**). Last, a number of sodium alkyl sulfinates and substituted aryl sulfinates all participated in the dual catalytic divergent protocol smoothly, delivering the desired sulfonyl-1,3-diene products with high yields and excellent regio- and *syn/anti*-selectivity (**45a–54a** & **45b–54b**).

To further demonstrate the synthetic applicability of this dual-protocol, late-stage modifications of complex molecules have been evaluated (Fig. 3a). Under the *syn*-selective conditions (entry 11, Table 1), the reaction of complex terminal alkynes or vinyl triflates, derived from estrone, indomethacin (anti-inflammatory), glucose, borneol, and amino acid, proceeded smoothly to afford the desired *E*-1,3-dienes with high yields and excellent stereoselectivity (**55a–59a**). Under the *anti*-selective condition (entry 2, Table 1), nevertheless, reactions with these complex substrates proceeded in comparable yields yet moderate stereoselectivity, probably due to the significant

steric hindrance of these complex substrates (**55b–59b**). Moreover, the resulting sulfonyl 1,3-dienes are useful building blocks in organic synthesis (Fig. 3b). Hydrogenation of **4b** in the presence of palladium on carbon (Pd/C) and H$_2$ gave alkyl sulfone **60** in 95% yield. Oxidation of **4b** with *m*-CPBA or KMnO$_4$ yielded epoxide **61** and polyol **62**, respectively. Furthermore, treatment of **4b** with *n*-butyllithium, followed by the addition of MeI, afforded 68% yield of (*Z*)-tetra-substituted sulfonyl alkene **63**, the stereoselective synthesis of which remains challenging. Cross-coupling of **4b** with methylmagnesium bromide in the presence of catalytic Ni(acac)$_2$ furnished (*E*)-tri-substituted 1,3-dienes **64** in 78% yield and excellent stereoselectivity. Finally, cycloaddition reactions of **4a** or **4b** with 4-phenyl-1,2,4-triazoline-3,5-dione (PTAD) **65** resulted in the formation of the two stereoisomers of products **66** and **66'** in moderate yields.

## Mechanistic studies

To gain insights into the potential mechanism, we have performed some preliminary mechanistic experiments (Fig. 4). On the one hand, we conducted a number of experiments regarding the photocatalytic part. Stern-Volmer fluorescence quenching studies indicated that the photoexcited *Ru(dtbbpy)$_3$$^{2+}$ was quenched by TsNa, other than alkyne **1** or vinyl triflate **2** (Fig. 4a). Light on/off experiments under both *anti*- and *syn*-selective conditions were performed, which showed that the desired couplings ceased in the dark (See Supplementary Figure 6–7); additionally, quantum yields (φ) of both *anti*- and *syn*-selective reactions were determined to be less than 1 (See Supplementary Information)[61]. These results ruled out the possibility of a radical chain pathway in this photochemical process. Furthermore, time-course studies of template reactions (phenylacetylene **1**, vinyl triflate **2**, and TsNa **3**) showed that *anti/syn*-selectivity of products **4a** and **4b** remained steady under the conditions shown in entries 2 or 11 (Fig. 4b). Additionally, no significant fluorescence quenching effect was observed between *E*-**4a** and photoexcited *Ru(dtbbpy)$_3$$^{2+}$ (E$_T$ ≈ 46 kcal/mol)[57] (Fig. 4a). These results precluded the involvement of
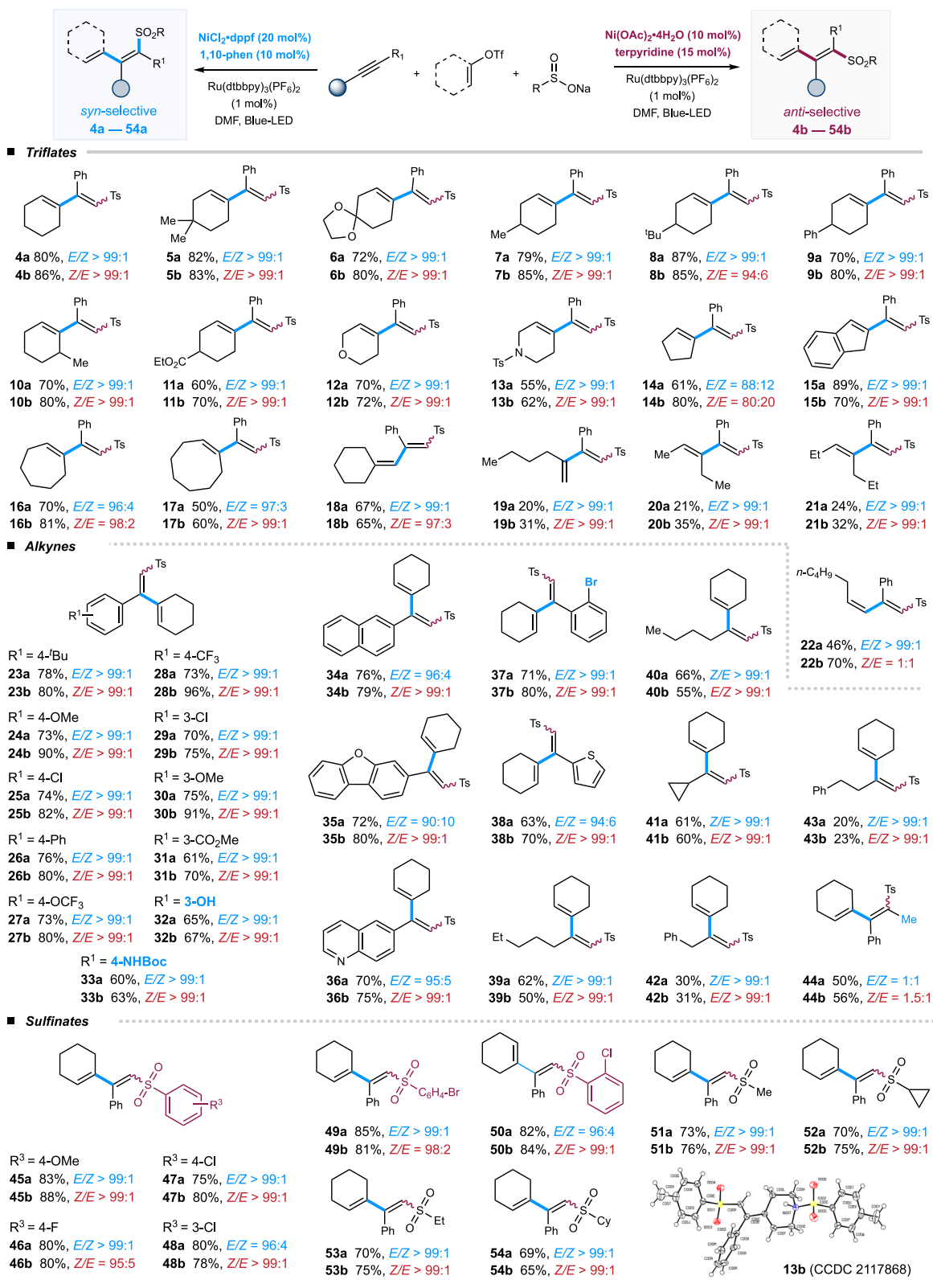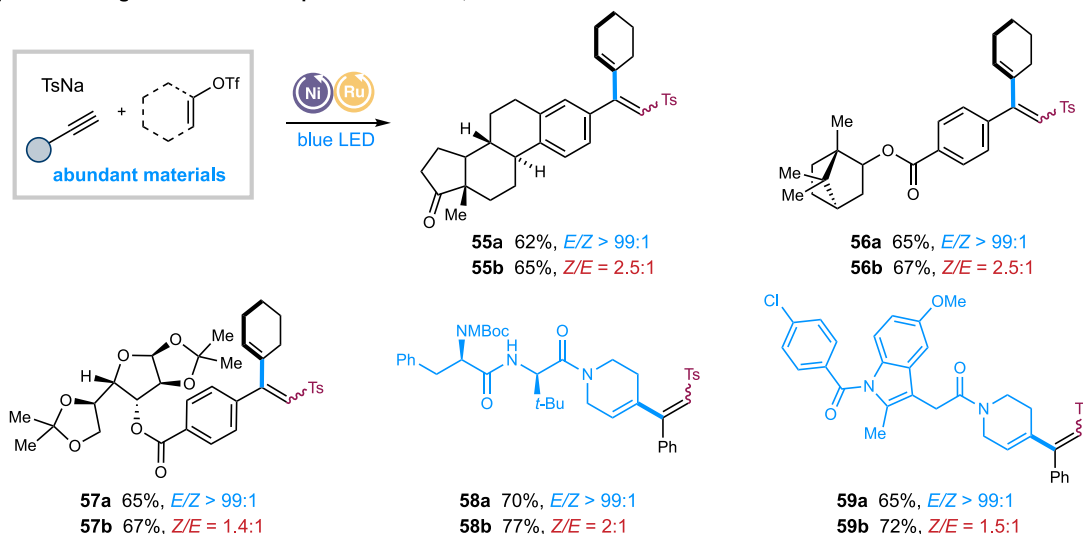
**Fig. 2 | Substrate Scope.** Reaction conditions: Ru(dtbbpy)₃(PF₆)₂ (1 mol%), Ni(OAc)₂•4H₂O/tpy (for *anti*-selective), NiCl₂•dppf/1,10-phen (for *syn*-selective), alkyne (1.5 equiv.), vinyl triflate (0.1 mmol), sodium sulfinate (1.5 equiv.), DMF [0.04 M], 35 °C, blue LED, 6 h. Isolated yields. Ts = toluenesulfonyl.

photocatalytic *E→Z* isomerization of sulfonyl 1,3-dienes, thus further supporting ligand control of stereoselectivity in this catalytic system[57]. On the other hand, we detected a small amount of side product ***E*-51** with careful monitoring of this reaction, implying that this reaction could proceed via sulfonyl addition followed by alkenylation (Fig. 4c).

Then, radical inhibition and probe reactions were performed (Figs. 4d-4e). The addition of 2,2,6,6-tetramethyl-1-piperidinyloxy (TEMPO) into the standard systems (entries 1 and 11, Table 1) completely shut down the desired reactions, while the addition of 1,1-diphenylethylene gave the desired products **4a/4b** in slightly decreased yields, together with a

**a) Stereodivergent access to complex sulfonated 1,3-dienes**



**55a** 62%, *E/Z* > 99:1
**55b** 65%, *Z/E* = 2.5:1

**56a** 65%, *E/Z* > 99:1
**56b** 67%, *Z/E* = 2.5:1

**57a** 65%, *E/Z* > 99:1
**57b** 67%, *Z/E* = 1.4:1

**58a** 70%, *E/Z* > 99:1
**58b** 77%, *Z/E* = 2:1

**59a** 65%, *E/Z* > 99:1
**59b** 72%, *Z/E* = 1.5:1

**b) Synthetic transformations of the resulting sulfonated 1,3-dienes**



**60** 95%

**61** 71% *E/Z* > 20: 1

**62** 74%

**63** 68% *Z/E* > 20: 1

**64** 80% *E/Z* > 20: 1

**65** (PTAD)

**66** 73%

**66'** 48% (from **4a**)
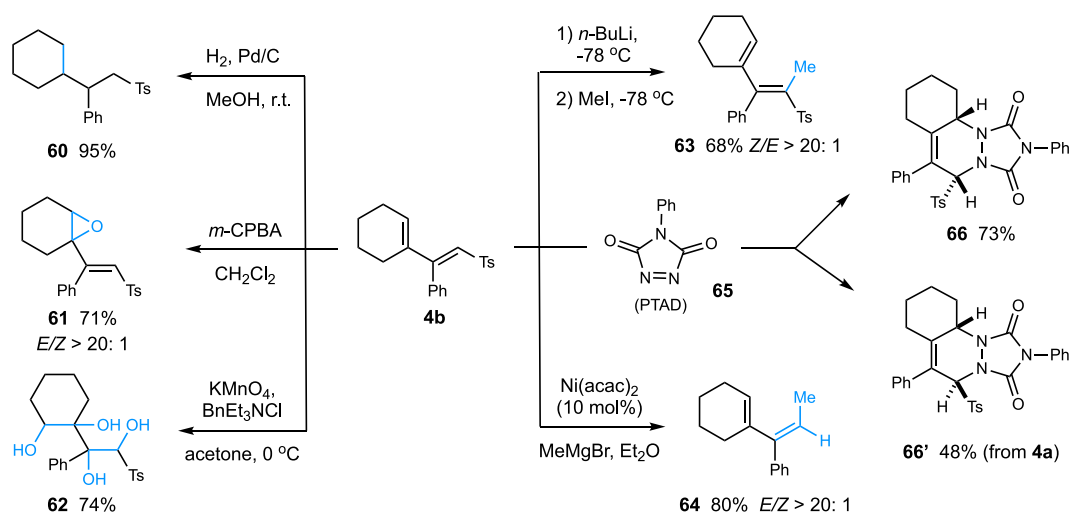
**Fig. 3 | Synthetic applications. a** Stereodivergent access to complex sulfonyl 1,3-dienes; **b** Synthetic transformations of sulfonyl 1,3-dienes. *m*-CPBA = *m*-chloroperoxybenzoic acid.

small amount of alkyl sulfone adduct **68** (Fig. 4d). Reaction of vinyl triflate **2** and TsNa with 1,5-diene **69**, instead of alkyne **1**, gave a small amount of tosylation/cyclization product **70** and tosylation/cyclization/alkenylation product **70'** under the *syn*-selective condition; interestingly, the parallel reaction under the *anti*-selective condition resulted in the formation of 9% yield of **70**, together with 71% yield of **70'** (Fig. 4e). These results implied that different reaction pathways could be involved in *syn*- and *anti*-selective systems. Additionally, control reactions with stoichiometric Ni(cod)$_2$ and dppf in the absence of 1,10-phen gave good yields of product **4a** (*Z/E* > 99:1), in contrast to the results with catalytic Ni(cod)$_2$/dppf (entry 7, Table 1), suggesting the importance of a synergistic effect with the two ligands (Fig. 4e)[62]. Furthermore, the reaction of alkyne **1**, alkenyl boronic acid **71**, and TsCl with catalytic NiCl$_2$(py)$_4$/tpy or NiCl$_2$•dppf/phen gave a small amount of *anti*-selective diene **4b** under thermal conditions[35], demonstrating the intriguing role of light irradiation in this stereodivergent alkenylation and further highlighting the synthetic advantage of this photochemical dual-protocol.

Next, we performed density functional theory (DFT) calculations to gain a deeper understanding of the mechanism and catalytic cycle,

particularly to rationalize the stereoselectivity controlled by the different ligands (Computational details are given in the supporting information) (Fig. 5). We chose **51a/b** as the model substrate with terpyridine and dppf/phenanthroline as the model ligands for the *anti/syn* selective conditions, respectively (Table 1, entries 3 and 11). In Fig. 5a, the Ni-catalytic cycle with terpyridine as the ligand begins with the Ni$^I$-SO$_2$Me intermediate **N1**[57]. First, phenylacetylene **1** coordinates to the intermediate **N1** and produces **N2**, followed by the rearrangement of the SO$_2$Me moiety from a Ni-S to Ni-O bonding mode with an energy barrier of 11.9 kcal/mol (**N2-3TS**). Two intermediates are formed in which the sulfonyl group is in a suitable orientation to either attack the terminal (**N3**) or internal (**N3'**) carbon of the alkyne. The sulfonyl group then migrates to the terminal carbon of the alkyne via a five-membered ring transition state (**N3-4ZTS**) with an energy barrier of 18.4 kcal/mol. In contrast, the migratory insertion into the internal carbon is disfavored by 3.0 kcal/mol (**N3'-4'TS**), which is consistent with the observed regioselectivity of this reaction. In the intermediate **N4Z**, the phenyl and sulfonyl moieties are *anti*-oriented after migratory insertion. Thus, it can either undergo direct S$_N$-Ar type of oxidative addition of vinyl triflate **2** via
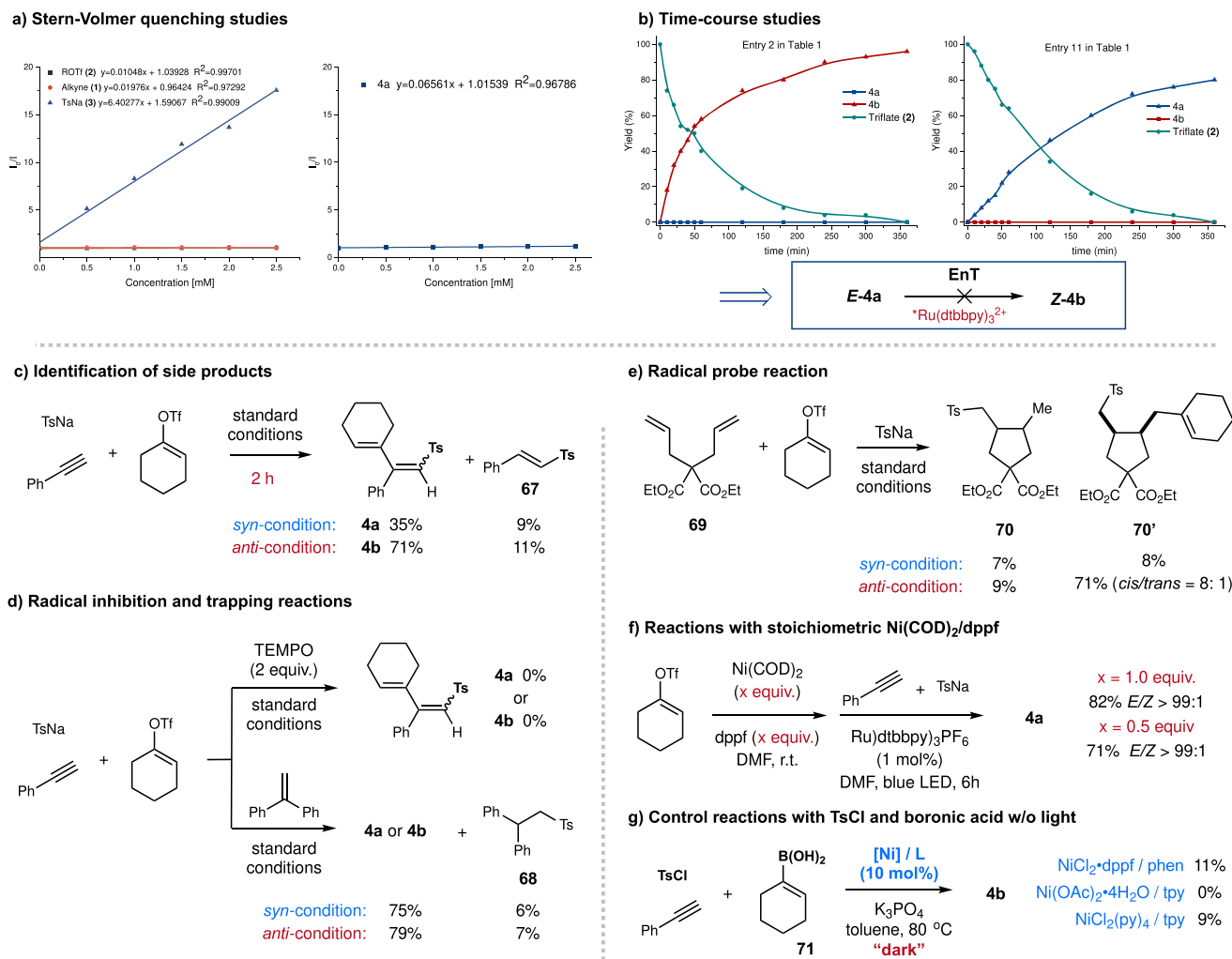
**Fig. 4 | Mechanistic studies. a** Stern-Volmer quenching studies; **b** Time-course studies; **c** Identification of side products; **d** Radical inhibition and trapping reactions; **e** Radical probe reaction; **f** Reaction with stoichiometric Ni(COD)₂/dppf; **g** Control reactions with TsCl and boronic acid w/o light. EnT = Energy transfer.

transition state **N4-5ZTS**, with an energy barrier of 31.6 kcal/mol, resulting in the *syn*-selective product **51b**, or undergo *anti*/*syn* isomerization followed by oxidative addition. The C-C bond rotates during the *anti*/*syn* isomerization with an activation energy of 25.1 kcal/mol, leading to the intermediate **N4E**. The $S_N$-Ar-type oxidative addition of vinyl triflate to **N4E** has an energy barrier of only 18.6 kcal/mol (**N4-5ETS**), which lies 8.7 kcal/mol below the transition state **N4-5ZTS**. The proximity of the sulfonyl and OTf groups in the transition state **N4-5ZTS** may account for the high oxidative addition energy barrier. A comparison of the two oxidative addition routes implies that the formation of *anti*-selective product **E** is preferred since the transition state **N4Z-ETS** is favored by 6.5 kcal/mol over **N4-5ZTS**, which explains the *anti*-stereoselectivity when terpyridine was used as the ligand. After the reductive elimination, the cross-coupling product is formed, together with the generation of the Ni[I] intermediate **N6**. The reduction of **N6** to Ni[0] intermediate **N8** by the Ru-photocatalyst is calculated to be thermodynamically disfavored (+2.2 kcal/mol, see Supplementary Figure 19). In contrast, the radical addition of sulfonyl radical to **N6** is barrierless, with an energy gain of 28.1 kcal/mol[63,64]. The generated Ni[II] intermediate **N7** can then be reduced by the Ru-photocatalyst and start the next catalytic cycle.

Subsequently, the reaction with a dual ligand system (dppf and phenanthroline) was explored, and the catalytic cycle is depicted in Fig. 5b. Based on a recent report[62], we proposed that the dynamic ligand exchanges on Ni intermediates promote different steps in the

*syn*-selective catalytic cycle. The phosphine ligand dppf facilitates the Ni[I] reduction and Ni[0] oxidative addition steps, while the phenanthroline ligand facilitates the radical addition step. The binding of vinyl triflate **2** to dppf-Ni[0] forms the intermediate **P1**, which undergoes $S_N$-Ar-type oxidative addition to afford the Ni[II] cation **P2** with an energy barrier of only 7.9 kcal/mol[65,66]. Next, the sulfonyl radical **R1** can either add to **P2** via the transition state **P2-5TS** with a 16.2 kcal/mol barrier, leading to **P5**, or add to the alkyne, forming the vinyl radical **R2**, with a barrier of 13.8 kcal/mol. The radical addition to an alkyne is kinetically and thermodynamically favored. The Ni[II] cation **P2** then undergoes ligand exchange with phenanthroline to afford Ni[II] intermediate **Phen1**. The vinyl radical **R2** undergoes radical addition with two distinct orientations to the Ni[II] cation **Phen1**, resulting in an *anti*-or *syn*-selective Ni[III] intermediate (**Phen2E** or **Phen2Z**). The transition state of the *syn*-selective radical addition is 14.1 kcal/mol (**Phen1-2ZTS**), favored by 7.3 kcal/mol over the *anti*-selective radical addition (**Phen1-2ETS**), which may be due to the coordination of the oxygen atom from the sulfonyl group to the Ni[II] metal center. Also, the *syn*-selective Ni[III] intermediate **Phen2Z** is more stable than the *anti*-selective Ni[III] intermediate **Phen2E** (15.9 kcal/mol difference in energy). With a barrier of only 3.5 kcal/mol, the reductive elimination of **Phen2Z** is rapid, yielding the *syn*-selective product. The resulting Ni[I] cation **Phen3** again undergoes ligand exchange with dppf to afford the dppf-Ni[I] intermediate **P4**. In contrast to the tpy-Ni[I] intermediate **N6**, the intermediate **P4** can easily be reduced by the Ru-photocatalyst, leading to
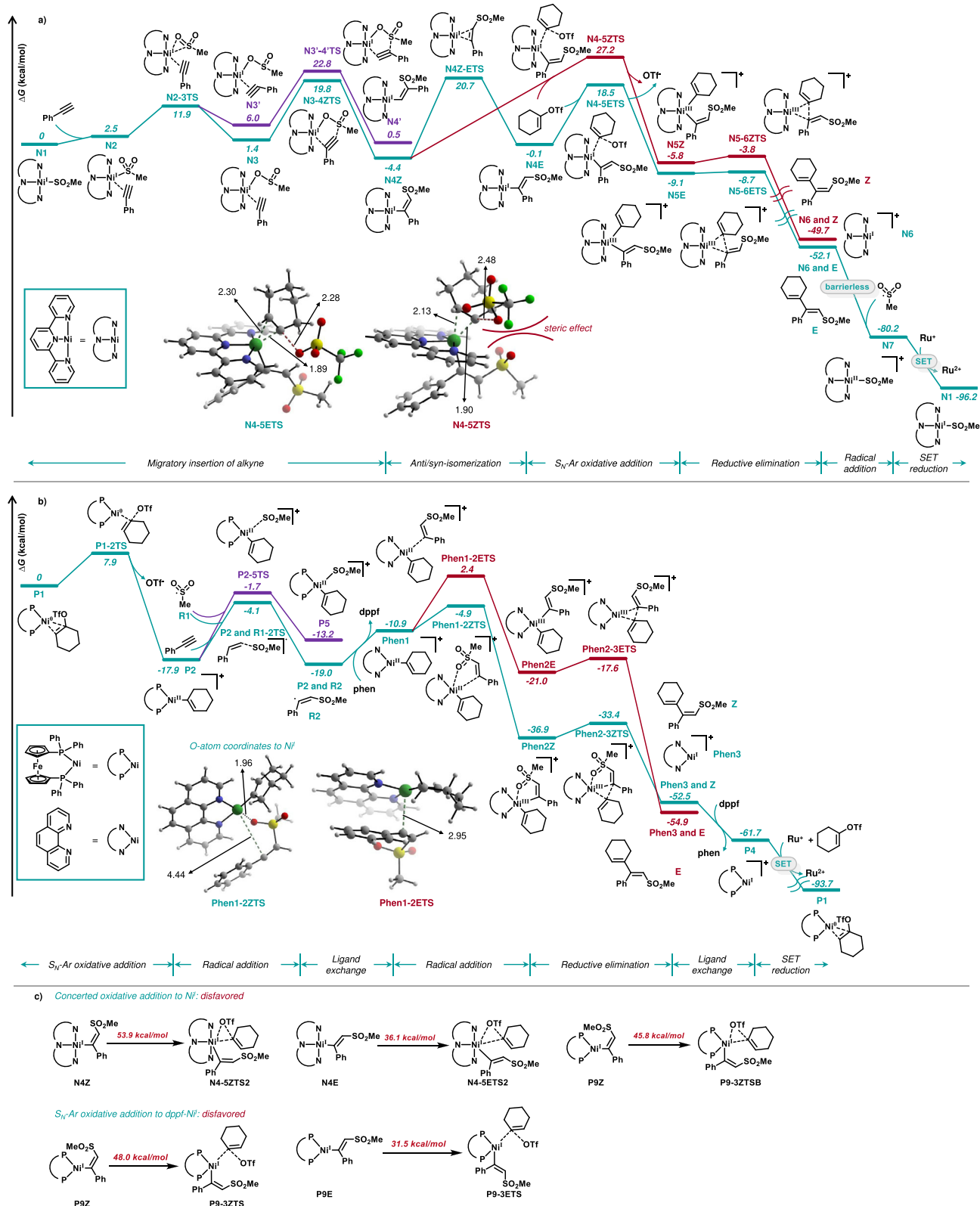
**Fig. 5 | DFT calculations. a** DFT-computed energy profiles for the sulfonylalk-enylation with terpyridine ligand. **b** DFT-computed energy profiles for the sulfo-nylalkenylation with dppf and phenanthroline ligand. **c** Energy barriers of concerted oxidative addition to Ni[I] and S$_N$-Ar oxidative addition to Ni[I] with dppf ligand. Free energies in solution (in kcal·mol^{-1}) were calculated at SMD (DMF)-M06/Def2-TZVPP//PBE-D3(BJ)/Def2-TZVP (Ni, Fe, Ru)/Def2-SVP (other atoms). DFT-optimized geometries of selected transition states or intermediates are shown. Bond lengths are in Å.
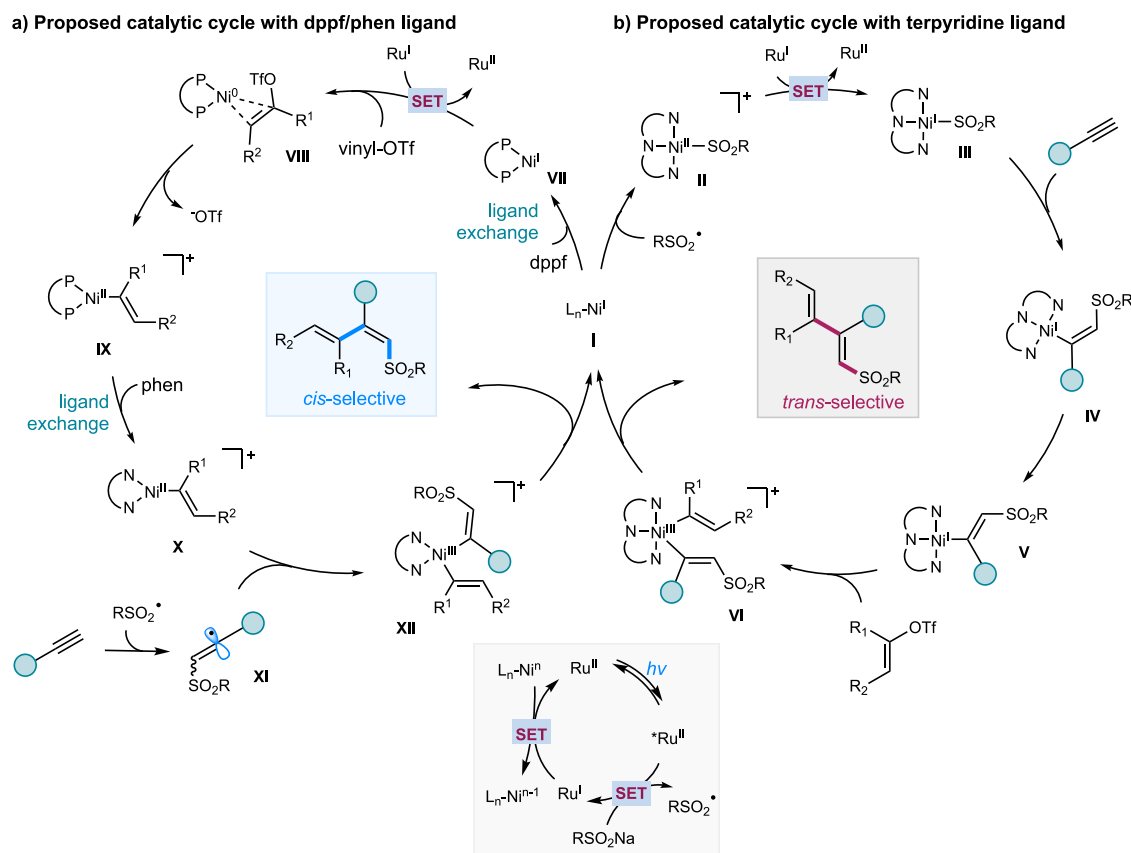
**Fig. 6 | Proposed reaction pathways. a** Proposed catalytic cycle with dppf/phen ligand. **b** Proposed catalytic cycle with terpydine ligand. dppf = 1,1-bis(diphenylpho-sphino)ferrocene; phen = 1,10-phenanthroline. $h\nu$ = visible light. SET = single electron transfer.

the formation of Ni$^0$ intermediate **P1** with an energy gain of 32.0 kcal/mol. The concerted oxidative addition to Ni$^i$ intermediate via a three-membered ring transition state was calculated to be disfavored. In addition, the S$_N$-Ar type oxidative addition to the dppf-Ni$^i$ intermediate is not feasible at room temperature for both *anti-* and *syn*-selective pathways (Fig. 5c). Given that 32% *syn*-selective product was obtained when only dppf was used as the ligand (see Table 1, entry 7), the *syn*-selective catalytic cycle with only dppf as the ligand was also explored (see Supplementary Figure 15 for the energy profile). The stereo-selectivity can also be explained by the 19.1 kcal/mol energy difference between the *anti/syn* radical addition step (**P2-3ZTS** *vs.* **P2-3ETS**). Alternatively, another catalytic pathway involving the migratory insertion of alkyne to dppf-ligated vinyl-Ni species was investigated, in which the regio- and stereoselectivity can also be explained (See Supplementary Figure 16 for the energy profile). However, this path-way was not chosen as the main catalytic pathway due to the observed hydrosulfonylation by-product **51** (Fig. 4c), which cannot be generated by this pathway.

Based on these experimental and computational results, we propose a plausible reaction pathway as depicted in Fig. 6. Upon light excitation, photoexcited *Ru(dtbbpy)$_3$$^{2+}$ ($E_{1/2}$$^{*ox}$ = +0.81 V vs. SCE)[67,68] interacts with RSO$_2$Na (TsNa, $E^{red}$ = + 0.45 V versus SCE in CH$_3$CN)[69] to release sulfonyl radical and the reducing Ru(I). In the case of ter-pyridine as ligand, the sulfonyl radical is trapped by Ni(I) **I** to give RSO$_2$-Ni(II) **II**[57], which is then single-electron reduced by Ru(I) to generate RSO$_2$-Ni(I) **II**. Migratory insertion of **II** into alkyne **III** regioselectively delivers *cis*-alkenylNi(I) species **IV**, followed by iso-merization, to afford the *trans*-alkenylNi(I) **V**. S$_N$-Ar type oxidative addition of **V** with vinyl triflate affords *trans*-Ni(III) **VI**, followed by reductive elimination, to furnish *anti*-addition dienes. In the case of

NiCl$_2$•dppf/phen, which is more electron-rich and less sterically hin-dered compared to NiCl$_2$(py)$_4$/tpy, dppf-ligated Ni(I) **VII** is more prone to a SET reduction by Ru(I) to generate Ni(0) species, followed by binding and facile S$_N$-Ar type oxidative addition with vinyl triflate to form dppf-ligated alkenylNi(II) **IX**. Then, **IX** undergoes ligand exchange with 1,10-phen to form phen-ligated alkenylNi(II) **X**. At the same time, the sulfonyl radical adds to alkyne to form vinyl radical **XI**, which is subsequently captured by phen-ligated alkenylNi(II) **X** to generate the more stable *cis*-Ni(III) species **XII**. Reductive elimination of Ni(III) **XII** furnishes *syn*-selective product as well as Ni(I) **I**, the latter of which undergoes ligand exchange with dppf to yield (dppf)Ni(I) **VII**. Finally, Ru(I) (Ru(dtbbpy)$_3$$^+$, $E_{1/2}$$^{II/I}$ = −1.45 V vs SCE)[67] is fea-sible to reduce (dppf)Ni(I) **VII** or (terpy)Ni(II) **II** [$E_{1/2}$ (Ni$^{II}$/Ni$^0$) = −1.2 V versus SCE in DMF][70] to regenerate the ground state Ru(dtbbpy)$_3$$^{2+}$ and close the two catalytic cycles.

In summary, we have developed a dual photoredox and nickel catalyzed stereodivergent three-component alkenyl-functionalization of alkynes with vinyl triflates and sodium sulfinates under mild and operationally simple conditions. Such a photochemical dual strategy enables divergent and straightforward access to *syn-* and *anti*-selective sulfonyl-1,3-dienes by a simple choice of nickel catalyst and ligand without the reliance on the structures of photocatalyst and alkene products. This method demonstrates broad substrate scope and excellent chemo-, regio-, and stereo-selectivity, with potential appli-cations in late-stage functionalizations. A series of mechanistic experiments, including Stern-Volmer fluorescence quenching studies, light on/off experiments, determination of quantum yields, radical probe reactions, and time course studies, as well as detailed compu-tational investigations, offer insights into the origins of the observed stereoselectivity controlled by simple ligands.

## Methods

### General procedure for the cis-selective alkenylation

To a flame-dried 8 mL reaction vial equipped with a magnetic stir bar was charged with Ru(dtbbpy)$_3$(PF$_6$)$_2$ (1 mol %), NiCl$_2$•dppf (20 mol %), 1,10-phenanthrane (10 mol %), sulfinate (1.5 equiv.), and DMF [0.04 M]. The reaction mixture was degassed by nitrogen sparging for 30 min, followed by the addition of vinyl triflate (0.10 mmol) and alkyne (1.5 equiv). The reaction mixture was irradiated with blue LEDs for 6 h (around 35 °C, with a cooling fan placed on the top of the vial). The reaction mixture was quenched with water and extracted with ethyl acetate. The combined organic layers were dried with MgSO$_4$, filtered and concentrated in vacuo. The crude material was purified by flash chromatography (silica gel, petroleum ether/ ethyl acetate) to afford the products.

### General procedures for the trans-selective alkenylation

To a flame-dried 8 mL reaction vial equipped with a magnetic stir bar was charged with Ru(dtbbpy)$_3$(PF$_6$)$_2$ (1 mol %), Ni(OAc)$_2$• 4H$_2$O (10 mol %), terpyridine (10 mol %), sulfinate (1.5 equiv.) and DMF [0.04 M]. The reaction mixture was degassed by nitrogen sparging for 30 min, followed by the addition of vinyl triflate (0.10 mmol) and alkyne (1.5 equiv.). Then the reaction mixture was irradiated with blue LEDs for 6 h (around 35 °C). The reaction mixture was quenched with water and extracted with ethyl acetate. The combined organic layers were dried with MgSO$_4$, filtered and concentrated in vacuo. The crude material was purified by flash chromatography (silica gel, petroleum ether/ ethyl acetate) to afford the products.

## Data availability

The data supporting the findings of this study are available within the paper and its Supplementary Information. Supplementary Data file 1 contains the cartesian coordinates of the calculated structures. The crystallographic data for the structures reported in this Article have been deposited at the Cambridge Crystallographic Data Centre, under deposition numbers CCDC 2117868 and 2117869. Copies of the data can be obtained free of charge via https://www.ccdc.cam.ac.uk/structures/.

## References

1. Rawal, V. H., Kozmin, S. A., Trost, B. M. & Abell, A. D. (Georg Thieme Verlag KG, 2009).
2. Harned, A. M. & Volp, K. A. The sorbicillinoid family of natural products: Isolation, biosynthesis, and synthetic studies. *Nat. Prod. Rep.* **28**, 1790–1810 (2011).
3. Reymond, S. & Cossy, J. Copper-Catalyzed Diels–Alder Reactions. *Chem. Rev.* **108**, 5359–5406 (2008).
4. Chen, J.-R., Hu, X.-Q., Lu, L.-Q. & Xiao, W.-J. Formal [4+1] Annulation Reactions in the Synthesis of Carbocyclic and Heterocyclic Systems. *Chem. Rev.* **115**, 5301–5365 (2015).
5. De Paolis, M., Chataigner, I. & Maddaluno, J. in *Top. Curr. Chem* (ed Jianbo Wang) 87-146 (Springer Berlin Heidelberg, 2012).
6. Hubert, P., Seibel, E., Beemelmanns, C., Campagne, J.-M. & de Figueiredo, R. M. Stereoselective Construction of (E,Z)-1,3-Dienes and Its Application in Natural Product Synthesis. *Adv. Synth. Catal.* **362**, 5532–5575 (2020).
7. Soengas, R. G. & Rodríguez-Solla, H. Modern Synthetic Methods for the Stereoselective Construction of 1,3-Dienes. *Molecules* **26**, 249 (2021).
8. Maryanoff, B. E. & Reitz, A. B. The Wittig olefination reaction and modifications involving phosphoryl-stabilized carbanions. Stereochemistry, mechanism, and selected synthetic aspects. *Chem. Rev.* **89**, 863–927 (1989).
9. Negishi, E.-i et al. Recent Advances in Efficient and Selective Synthesis of Di-, Tri-, and Tetrasubstituted Alkenes via Pd-Catalyzed Alkenylation–Carbonyl Olefination Synergy. *Acc. Chem. Res.* **41**, 1474–1485 (2008).
10. Miyaura, N. & Suzuki, A. Palladium-Catalyzed Cross-Coupling Reactions of Organoboron Compounds. *Chem. Rev.* **95**, 2457–2483 (1995).
11. Diver, S. T. & Giessert, A. J. Enyne Metathesis (Enyne Bond Reorganization). *Chem. Rev.* **104**, 1317–1382 (2004).
12. Hou, C.-J., Schuppe, A. W., Knippel, J. L., Ni, A. Z. & Buchwald, S. L. A Dual CuH- and Pd-Catalyzed Stereoselective Synthesis of Highly Substituted 1,3-Dienes. *Org. Lett.* **23**, 8816–8821 (2021).
13. Stille, J. K. & Groh, B. L. Stereospecific cross-coupling of vinyl halides with vinyl tin reagents catalyzed by palladium. *J. Am. Chem. Soc.* **109**, 813–817 (1987).
14. Stefani, H. A., Guarezemini, A. S. & Cella, R. Homocoupling reactions of alkynes, alkenes and alkyl compounds. *Tetrahedron* **66**, 7871–7918 (2010).
15. Fiorito, D., Folliet, S., Liu, Y. & Mazet, C. A General Nickel-Catalyzed Kumada Vinylation for the Preparation of 2-Substituted 1,3-Dienes. *ACS Catal.* **8**, 1392–1398 (2018).
16. Vázquez-Galiñanes, N. & Fañanás-Mastral, M. Stereoselective Synthesis of Borylated 1,3-Dienes by Synergistic Cu/Pd Catalysis. *ChemCatChem* **10**, 4817–4820 (2018).
17. Dutta, S. et al. Cationic-palladium catalyzed regio- and stereoselective syn-1,2-dicarbofunctionalization of unsymmetrical internal alkynes. *Nat. Commun.* **13**, 1360 (2022).
18. Xu, W.-Y., Li, Y.-J., Gong, T.-J. & Fu, Y. Synthesis of gem-Difluorinated 1,3-Dienes via Synergistic Cu/Pd-Catalyzed Borodifluorovinylation of Alkynes. *Org. Lett.* **24**, 5884–5889 (2022).
19. Vanjari, R., Dutta, S., Yang, S., Gandon, V. & Sahoo, A. K. Palladium-Catalyzed Regioselective Arylalkenylation of Ynamides. *Org. Lett.* **24**, 1524–1529 (2022).
20. Kazem Shiroodi, R., Dudnik, A. S. & Gevorgyan, V. Stereocontrolled 1,3-Phosphatyloxy and 1,3-Halogen Migration Relay toward Highly Functionalized 1,3-Dienes. *J. Am. Chem. Soc.* **134**, 6928–6931 (2012).
21. Dang, H. T. et al. Z-Selective Dienylation Enables Stereodivergent Construction of Dienes and Unravels a Ligand-Driven Mechanistic Dichotomy. *ACS Catal.* **11**, 1042–1052 (2021).
22. Montgomery, J. Nickel-Catalyzed Cyclizations, Couplings, and Cycloadditions Involving Three Reactive Components. *Acc. Chem. Res.* **33**, 467–473 (2000).
23. Besset, T., Poisson, T. & Pannecoucke, X. Direct Vicinal Difunctionalization of Alkynes: An Efficient Approach Towards the Synthesis of Highly Functionalized Fluorinated Alkenes. *Eur. J. Org. Chem.* **2015**, 2765–2789 (2015).
24. Liu, W. & Kong, W. Ni-Catalyzed stereoselective difunctionalization of alkynes. *Org. Chem. Front.* **7**, 3941–3955 (2020).
25. Corpas, J., Mauleón, P., Arrayás, R. G. & Carretero, J. C. Transition-Metal-Catalyzed Functionalization of Alkynes with Organoboron Reagents: New Trends, Mechanistic Insights, and Applications. *ACS Catal.* **11**, 7513–7551 (2021).
26. Zhu, S., Zhao, X., Li, H. & Chu, L. Catalytic three-component dicarbofunctionalization reactions involving radical capture by nickel. *Chem. Soc. Rev.* **50**, 10836–10856 (2021).
27. Huggins, J. M. & Bergman, R. G. Mechanism, regiochemistry, and stereochemistry of the insertion reaction of alkynes with methyl(2,4-pentanedionato)(triphenylphosphine)nickel. A cis insertion that leads to trans kinetic products. *J. Am. Chem. Soc.* **103**, 3002–3011 (1981).
28. Yamamoto, A. & Suginome, M. Nickel-Catalyzed trans-Alkynylboration of Alkynes via Activation of a Boron–Chlorine Bond. *J. Am. Chem. Soc.* **127**, 15706–15707 (2005).
29. Daini, M., Yamamoto, A. & Suginome, M. Nickel-Catalyzed Cyclizativetrans-Carboboration of Alkynes through Activation of Boron-

Chlorine Bonds by Using Organometallic Reagents as Donors of Organic Groups. *Asian J. Org. Chem.* **2**, 968–976 (2013).

30. Clarke, C., Incerti-Pradillos, C. A. & Lam, H. W. Enantioselective Nickel-Catalyzed anti-Carbometallative Cyclizations of Alkynyl Electrophiles Enabled by Reversible Alkenylnickel E/Z Isomerization. *J. Am. Chem. Soc.* **138**, 8068–8071 (2016).

31. Zhang, X., Xie, X. & Liu, Y. Nickel-catalyzed cyclization of alkyne-nitriles with organoboronic acids involving anti-carbometalation of alkynes. *Chem. Sci.* **7**, 5815–5820 (2016).

32. Yap, C. et al. Enantioselective Nickel-Catalyzed Intramolecular Allylic Alkenylations Enabled by Reversible Alkenylnickel E/Z Isomerization. *Angew. Chem. Int. Ed.* **56**, 8216–8220 (2017).

33. Lu, Z. et al. Enantioselective Assembly of Cycloenones with a Nitrile-Containing All-Carbon Quaternary Center from Malononitriles Enabled by Ni Catalysis. *J. Am. Chem. Soc.* **142**, 7328–7333 (2020).

34. Bottcher, S. E., Hutchinson, L. E. & Wilger, D. J. Nickel-Catalyzed anti-Selective Alkyne Functionalization Reactions. *Synthesis* **52**, 2807–2820 (2020).

35. Li, Z., García-Domínguez, A. & Nevado, C. Nickel-Catalyzed Stereoselective Dicarbofunctionalization of Alkynes. *Angew. Chem. Int. Ed.* **55**, 6938–6941 (2016).

36. García-Domínguez, A., Müller, S. & Nevado, C. Nickel-Catalyzed Intermolecular Carbosulfonylation of Alkynes via Sulfonyl Radicals. *Angew. Chem. Int. Ed.* **56**, 9949–9952 (2017).

37. Rawner, T., Lutsker, E., Kaiser, C. A. & Reiser, O. The Different Faces of Photoredox Catalysts: Visible-Light-Mediated Atom Transfer Radical Addition (ATRA) Reactions of Perfluoroalkyl Iodides with Styrenes and Phenylacetylenes. *ACS Catal.* **8**, 3950–3956 (2018).

38. Jiang, Y., Pan, J., Yang, T., Zhao, Y. & Koh, M. J. Nickel-catalyzed site- and stereoselective reductive alkylalkynylation of alkynes. *Chem* **7**, 993–1005 (2021).

39. Maiti, S. & Rhlee, J. H. Reductive Ni-catalysis for stereoselective carboarylation of terminal aryl alkynes. *Chem. Commun.* **57**, 11346–11349 (2021).

40. Zhan, Y.-Z., Xiao, N. & Shu, W. Ni-catalyzed regio- and stereodefined intermolecular cross-electrophile dialkylation of alkynes without directing group. *Nat. Commun.* **12**, 928 (2021).

41. Dai, Y., Wang, F., Zhu, S. & Chu, L. Selective Ni-catalyzed cross-electrophile coupling of alkynes, fluoroalkyl halides, and vinyl halides. *Chin. Chem. Lett.* **33**, 4074–4078 (2022).

42. Li, H., Wang, F., Zhu, S. & Chu, L. Selective Fluoromethyl Couplings of Alkynes via Nickel Catalysis. *Angew. Chem. Int. Ed.* **61**, e202116725 (2022).

43. Gui, Y.-Y., Sun, L., Lu, Z.-P. & Yu, D.-G. Photoredox sheds new light on nickel catalysis: from carbon–carbon to carbon–heteroatom bond formation. *Org. Chem. Front.* **3**, 522–526 (2016).

44. Twilton, J. et al. The merger of transition metal and photocatalysis. *Nat. Rev. Chem.* **1**, 0052 (2017).

45. Milligan, J. A., Phelan, J. P., Badir, S. O. & Molander, G. A. Alkyl Carbon–Carbon Bond Formation by Nickel/Photoredox Cross-Coupling. *Angew. Chem. Int. Ed.* **58**, 6152–6163 (2019).

46. Zhu, C., Yue, H., Chu, L. & Rueping, M. Recent advances in photoredox and nickel dual-catalyzed cascade reactions: pushing the boundaries of complexity. *Chem. Sci.* **11**, 4051–4064 (2020).

47. Chan, A. Y. et al. Metallaphotoredox: The Merger of Photoredox and Transition Metal Catalysis. *Chem. Rev.* **122**, 1485–1542 (2022).

48. Deng, H.-P., Fan, X.-Z., Chen, Z.-H., Xu, Q.-H. & Wu, J. Photoinduced Nickel-Catalyzed Chemo- and Regioselective Hydroalkylation of Internal Alkynes with Ether and Amide α-Hetero C(sp3)–H Bonds. *J. Am. Chem. Soc.* **139**, 13579–13584 (2017).

49. Guo, L., Song, F., Zhu, S., Li, H. & Chu, L. syn-Selective alkylarylation of terminal alkynes via the combination of photoredox and nickel catalysis. *Nat. Commun.* **9**, 4543 (2018).

50. Till, N. A., Smith, R. T. & MacMillan, D. W. C. Decarboxylative Hydroalkylation of Alkynes. *J. Am. Chem. Soc.* **140**, 5701–5705 (2018).

51. Yue, H., Zhu, C., Kancherla, R., Liu, F. & Rueping, M. Regioselective Hydroalkylation and Arylalkylation of Alkynes by Photoredox/Nickel Dual Catalysis: Application and Mechanism. *Angew. Chem. Int. Ed.* **59**, 5738–5746 (2020).

52. Zhao, X. et al. Divergent Aminocarbonylations of Alkynes Enabled by Photoredox/Nickel Dual Catalysis. *Angew. Chem. Int. Ed.* **60**, 26511–26517 (2021).

53. Xu, L. et al. Radical 1,2-addition of bromoarenes to alkynes via dual photoredox and nickel catalysis. *Org. Chem. Front.* **8**, 2924–2931 (2021).

54. Yu, W., Jiao, X., Fan, Y., Zhu, S. & Chu, L. Metallaphotoredox-Enabled Intermolecular Carbobromination of Alkynes with Alkenyl Bromides. *Adv. Synth. Catal.* **364**, 1239–1244 (2022).

55. Zhu, C., Yue, H. & Rueping, M. Nickel catalyzed multicomponent stereodivergent synthesis of olefins enabled by electrochemistry, photocatalysis and photo-electrochemistry. *Nat. Commun.* **13**, 3240 (2022).

56. Zhao, T.-T. et al. Photoredox/nickel dual catalyzed stereospecific synthesis of distal alkenyl ketones. *Chem. Commun.* **58**, 1171–1174 (2022).

57. Zhu, C. et al. A multicomponent synthesis of stereodefined olefins via nickel catalysis and single electron/triplet energy transfer. *Nat. Catal.* **2**, 678–687 (2019).

58. Bäckvall, J.-E., Chinchilla, R., Nájera, C. & Yus, M. The Use of Sulfonyl 1,3-Dienes in Organic Synthesis. *Chem. Rev.* **98**, 2291–2312 (1998).

59. Back, T. G., Clary, K. N. & Gao, D. Cycloadditions and Cyclizations of Acetylenic, Allenic, and Conjugated Dienyl Sulfones. *Chem. Rev.* **110**, 4498–4553 (2010).

60. Greaves, M. E., Ronson, T. O., Maseras, F. & Nelson, D. J. The Effect of Added Ligands on the Reactions of [Ni(COD)(dppf)] with Alkyl Halides: Halide Abstraction May Be Reversible. *Organometallics* **40**, 1997–2007 (2021).

61. Kaga, A. et al. Degenerative xanthate transfer to olefins under visible-light photocatalysis. *Beilstein J. Org. Chem.* **14**, 3047–3058 (2018).

62. Hamby, T. B., LaLama, M. J. & Sevov, C. S. Controlling Ni redox states by dynamic ligand exchange for electroreductive Csp3–Csp2 coupling. *Science* **376**, 410–416 (2022).

63. Oderinde, M. S., Frenette, M., Robbins, D. W., Aquila, B. & Johannes, J. W. Photoredox Mediated Nickel Catalyzed Cross-Coupling of Thiols With Aryl and Heteroaryl Iodides via Thiyl Radicals. *J. Am. Chem. Soc.* **138**, 1760–1763 (2016).

64. Maity, B. et al. Mechanistic Insight into the Photoredox-Nickel-HAT Triple Catalyzed Arylation and Alkylation of α-Amino Csp3–H Bonds. *J. Am. Chem. Soc.* **142**, 16942–16952 (2020).

65. Bajo, S., Laidlaw, G., Kennedy, A. R., Sproules, S. & Nelson, D. J. Oxidative Addition of Aryl Electrophiles to a Prototypical Nickel(0) Complex: Mechanism and Structure/Reactivity Relationships. *Organometallics* **36**, 1662–1672 (2017).

66. Liu, R. Y., Dennis, J. M. & Buchwald, S. L. The Quest for the Ideal Base: Rational Design of a Nickel Precatalyst Enables Mild, Homogeneous C–N Cross-Coupling. *J. Am. Chem. Soc.* **142**, 4500–4507 (2020).

67. Prier, C. K., Rankic, D. A. & MacMillan, D. W. C. Visible Light Photoredox Catalysis with Transition Metal Complexes: Applications in Organic Synthesis. *Chem. Rev.* **113**, 5322–5363 (2013).

68. van der Westhuizen, D., von Eschwege, K. G. & Conradie, J. Electrochemistry and spectroscopy of substituted [Ru(phen)3]2+ and [Ru(bpy)3]2+ complexes. *Electrochim. Acta* **320**, 134540 (2019).

69. Yue, H., Zhu, C. & Rueping, M. Cross-Coupling of Sodium Sulfinates with Aryl, Heteroaryl, and Vinyl Halides by Nickel/Photoredox Dual Catalysis. *Angew. Chem. Int. Ed.* **57**, 1371–1375 (2018).

70. Zuo, Z. et al. Merging photoredox with nickel catalysis: Coupling of α-carboxyl sp3-carbons with aryl halides. *Science* **345**, 437–440 (2014).

## Author contributions

L.C. and M.R. conceived this work. T.L., L.L., L.S., and S.Z. performed all of the experiments and analyzed all of the data. C.Z. performed the DFT calculations. L.C. and M.R. wrote the manuscript with input from T.L., C.Z., L.L., L.S., and S.Z.. T.L. and C.Z. contributed equally.

## Competing interests

The authors declare no competing interests.

## Additional information

**Supplementary information** The online version contains supplementary material available at https://doi.org/10.1038/s41467-022-35688-2.

**Correspondence** and requests for materials should be addressed to Magnus Rueping or Lingling Chu.

**Peer review information** *Nature Communications* thanks Akhila K. Sahoo, John Milligan and the other, anonymous, reviewer(s) for their contribution to the peer review of this work.

**Reprints and permissions information** is available at http://www.nature.com/reprints

**Publisher's note** Springer Nature remains neutral with regard to jurisdictional claims in published maps and institutional affiliations.